HETEROCYCLES, Vol. 101, No. 2, 2020, pp. 611 - 620. © 2020 The Japan Institute of Heterocyclic Chemistry
Received, 18th July, 2019, Accepted, 28th August, 2019, Published online, 25th September, 2019
DOI: 10.3987/COM-19-S(F)51

# 5-AMINO-2-THIAZOLYLPYRIDINE *N*-OXIDES: SYNTHESIS AND PROPERTIES

**Toshiaki Murai,* Yuuta Nakatsu, Yuki Tsuchiya, Kirara Yamaguchi, Toshifumi Maruyama, Yohei Miwa, and Shoichi Kutsumizu**

Department of Chemistry and Biomolecular Science, Faculty of Engineering, Gifu University, Yanagido, Gifu 501-1193, Japan. mtoshi@gifu-u.ac.jp

**Abstract** – 5-Amino-2-thiazolylpyridine *N*-oxides were prepared in low to moderate yields by the oxidation of 2-pyridyl-5-aminothiazoles with *m*-CPBA. The molecular structures of the resulting *N*-oxides were unequivocally determined by X-ray analyses. The *N*-oxides exhibited the absorption maxima at around 415 ± 20 nm in a $CHCl_3$ solution, while the emission spectra were observed in the range of 505 to 604 nm. The red-shift of the emission was attributed to the methoxy groups attached to the para-position of an aromatic group on the nitrogen atom at the 5-position. The *N*-oxides exhibited halochromism with the addition of $B(C_6F_5)_3$. The change in absorption implied the formation of a 1:1 complex between *N*-oxide and $B(C_6F_5)_3$. The emission wavelengths of the *N*-oxides were observed at 510 ± 25 nm in a solid state. Interestingly, one of the *N*-oxides having methoxy groups exhibited mechanofluorochromism. The solid-state emission of the *N*-oxide at 527 nm shifted to a longer wavelength (599 nm) when it was subjected to grinding.

## INTRODUCTION

As part of our studies on main group chemistry,[1] we recently developed 5-aminothiazoles[2] as new fluorescent molecules. Our 5-aminothiazoles are monocyclic D-π-A-type highly twisted molecules and that show emissions from blue to orange depending on the substituents on the amino groups and at the 2-position of thiazoles. Among them, 2-pyridyl-5-aminothiazoles showed stimuli-responsive changes in emissions. The addition of Lewis acids to the thiazoles shifted the emissions to longer wavelengths. Tuning of the ratio of the thiazoles and Lewis acids enabled white-light emissions.[3] In addition, the pyridinium salts of 2-pyridyl-5-aminothiazoles exhibited reversible vapochromism in response to

halogenated solvents.[4] These phenomena were achieved by introducing an electron-withdrawing group to the nitrogen atom on the pyridyl group. We then further envisioned that the introduction of pyridine *N*-oxide moieties as an electron-withdrawing group to thiazoles could give thiazoles that showed emissions at longer wavelengths.[5] We report herein the synthesis and properties of (5-amino-2-thiazolyl)pyrdine *N*-oxides. The resulting *N*-oxides show emission in a solid state, which is of great interest[6] because of their wide potential applicability, such as in organic electronics and bioimaging. Furthermore, one of the *N*-oxides exhibited mechanofluorochromism.

## RESULTS AND DISCUSSION

We prepared 2-pyridyl-5-*N*,*N*-diarylaminothiazoles by our previously developed method as starting materials for pyridine *N*-oxides (Scheme 1). Initially, secondary thioamides **1** were treated with a base followed by the addition of *N*,*N*-diarylthioformamides **2** and iodine to generate 5-aminothiazoles **3** without the formation of further oxidized products **4** (eq. 1). Oxidation of the isolated 5-aminothiazolines **3** with iodine gave the thiazoles **4** in moderate to good yields (eq. 2). Further oxidation of the resulting thiazoles **4** with *m*-CPBA led to the desired pyridine *N*-oxides **5** (eq. 3). According to the literature,[7] oxidation of the nitrogen atom in the pyridyl group generally proceeds smoothly. In contrast, oxidation of the pyridyl group of **4b**, **4c**, and **4d** required longer reaction times, and the oxidation of **4a** and **4c** gave the desired products **5a** and **5c** in low to moderate yields. Nevertheless, we obtained the pyridine *N*-oxides **5** in a pure form and further elucidated their properties.

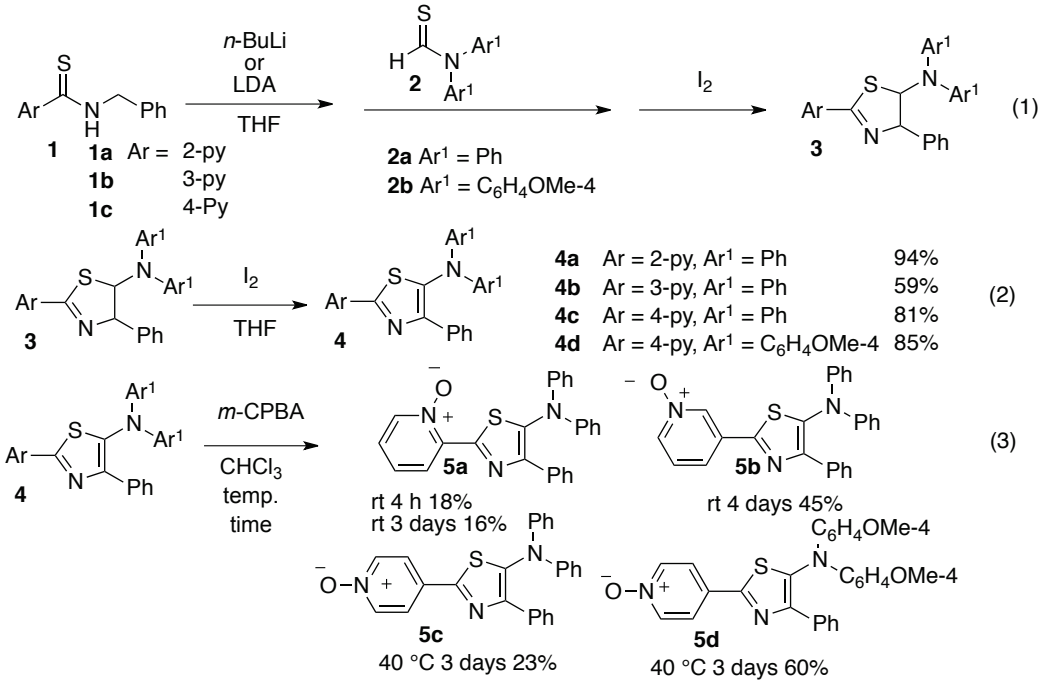


Scheme 1. Synthesis of pyridine *N*-oxides **5**

The structures of *N*-oxides **5** were unequivocally determined by X-ray crystal structure analyses of *N*-oxides **5a** and **5d**. Their ORTEP diagrams are shown in Figures 1 and 2. Oxidation of **5** evidently took place at the nitrogen atom of the pyridyl group despite the fact that thiazoles **4** possess three nitrogen atoms. The oxygen atom of pyridine *N*-oxide **5a** was oriented to the sulfur atom of the thiazole ring. As in the previously disclosed structures of 5-aminothiazoles,[2b] the pyridine *N*-oxide moieties and the phenyl group at the 4-position are nearly in the same plane as the thiazole rings, whereas *N*,*N*-diarylamino groups at the 5-position are highly deviated from the thiazole rings.

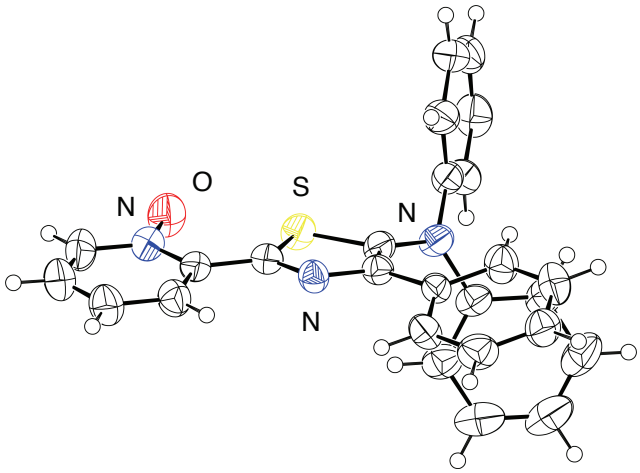


Figure 1. Molecular structure of thiazole **5a** (thermal ellipsoids set at 50% probability)

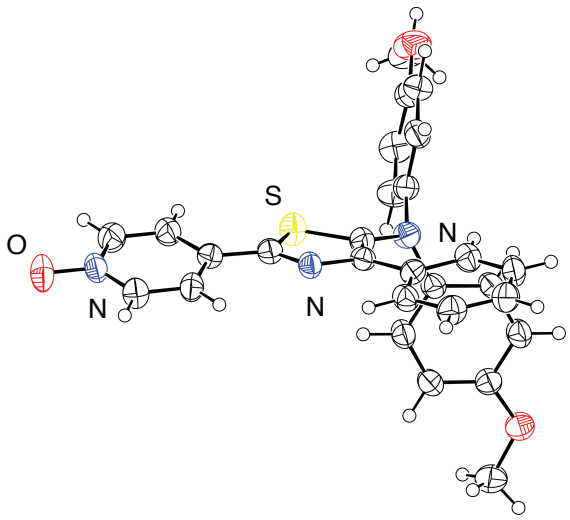


Figure 2. Molecular structure of thiazole **5d** (thermal ellipsoids set at 50% probability)

UV-visible and fluorescence spectral data for thiazoles **4** and pyridine *N*-oxides **5** in $CHCl_3$ are presented in Table 1 and Figures S1 and S2. The wavelengths of the absorption of **4** are shifted to longer wavelengths by 23±9 nm in the case of *N*-oxides **5**. Oxidation of the 2-pyridiyl group in **4a** had the greatest influence on the red-shift. Likewise, the emission of **5** was observed at longer wavelengths. In

particular, the fluorescence spectra of **5d**, wherein the methoxy group was attached at the para-position of the benzene ring on the nitrogen atom, exhibited emission at 604 nm with nearly the same intensity as that for **4d**.

Table 1. UV-vis and fluorescence spectra of thiazoles **4** and **5** in $CHCl_3$

| entry | Thiazole | UV-vis[a] | | Fluorescence[a,b] | | Stokes shift ($cm^{-1}$) [nm] |
|---|---|---|---|---|---|---|
| | | $\lambda_{abs\ max}$ (nm) | log ε | $\lambda_{em}$ (nm) | $\Phi_F$ | |
| 1 | 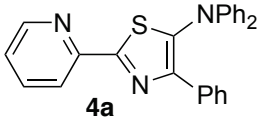 **4a** | 386 | 4.14 | 489 | 0.57 | 5457 (103) |
| 2 | 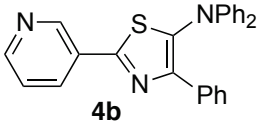 **4b** | 376 | 3.99 | 480 | 0.56 | 5762 (104) |
| 3 | 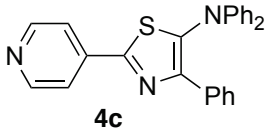 **4c** | 389 | 3.91 | 500 | 0.48 | 5707 (111) |
| 4 | 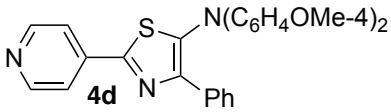 **4d** | 413 | 4.09 | 569 | 0.12 | 6638 (156) |
| 5 | 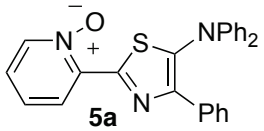 **5a** | 417 | 4.03 | 521 | 0.41 | 4787 (104) |
| 6 | 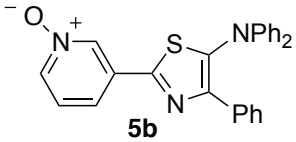 **5b** | 397 | 3.99 | 505 | 0.35 | 5387 (108) |
| 7 | 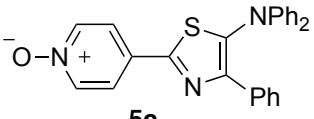 **5c** | 408 | 3.93 | 524 | 0.54 | 5426 (116) |
| 8 | 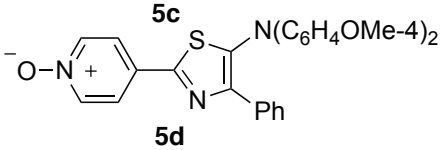 **5d** | 436 | 4.12 | 604 | 0.10 | 6380 (168) |

[a] In $CHCl_3$, [thiazole] = $1x10^{-5}$ M.
[b] Excited at $\lambda_{ex\ max}$. $\Phi_F$ corresponds to absolute fluorescence quantum yield.

The solvent effect of the absorption and emission spectra of **5c** was then elucidated (Table 2 and Figure S3). The absorption spectra of **5c** were almost independent of the solvent used and observed at around 400 nm. In contrast, emission of **5** shifted to longer wavelengths as the polarity of the solvent increased. The emission in methanol shifted to longer wavelengths by about 100 nm compared to that in toluene.

The Lippert-Mataga correlation[8] exhibited a linear relationship between orientational polarizability $\Delta f$ (as a function of solvent dielectric constant $\varepsilon$ and refractive index $n$) and Stokes shifts $\Delta\nu$ (Figure 3). Therefore, a solvent effect is present in the excited state. This further implies that the excitation of **5** proceeds via an intramolecular charge transfer mechanism. In the ground state shown in Figures 1 and 2, *N*-oxides **5** adopt highly deviated structures. Therefore, their excitation may involve a planarized intramolecular charge transfer process.[9]

Table 2. Solvatochromism of thiazole **5c**

| Thiazole | | toluene | THF | $CHCl_3$ | $CH_2Cl_2$ | MeCN | MeOH |
|---|---|---|---|---|---|---|---|
| | $E_T(30)$ | 33.9 | 37.4 | 39.1 | 40.7 | 45.6 | 55.4 |
| 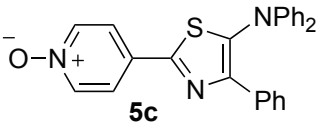 **5c** | $\lambda_{abs}$ (nm)[a] | 398 | 390 | 408 | 398 | 397 | 410 |
| | log$\varepsilon$ | 4.00 | 4.09 | 3.93 | 4.15 | 4.14 | 3.90 |
| | $\lambda_{em}$ (nm)[a,b] | 488 | 507 | 524 | 525 | 541 | 580 |
| | $\Phi_F$ | 0.06 | 0.11 | 0.54 | 0.44 | 0.32 | 0.15 |
| | Stokes shift | | | | | | |
| | ($cm^{-1}$) | 4634 | 5917 | 5426 | 6078 | 6705 | 7149 |
| | (nm) | 90 | 117 | 116 | 127 | 144 | 170 |

[a] In $CHCl_3$, [thiazole] = $1x10^{-5}$ M.
[b] Excited at $\lambda_{ex\ max}$. $\Phi_F$ corresponds to absolute fluorescence quantum yield.

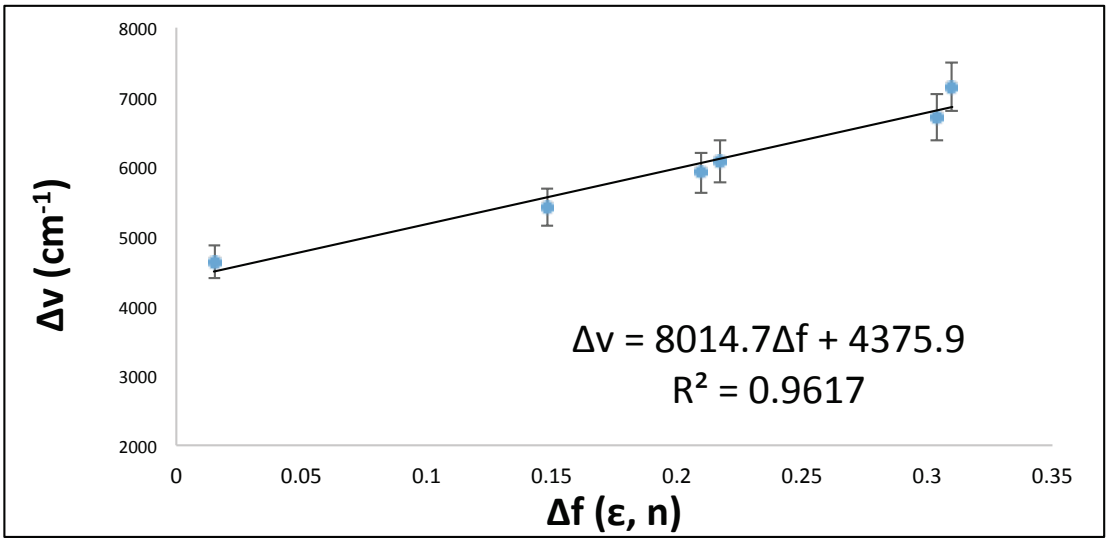


Figure 3. The Lippert-Mataga plot of **5c** in solvents of different polarities

The acid-responsive change in the spectra of **5c** was then examined since compounds **5** possess a Lewis basic oxygen atom. The development of fluorescent molecules showing acid-responsive chromism, which has been called halochromism,[10] is of paramount interest since this phenomenon can achieve white-light emission with a single fluorescent molecule and multiple excited-state molecules by combining with acids.[11] The results are shown in Table 3 and Figures S4–S6. When $B(C_6F_5)_3$ was added to a toluene solution of **5c**, the maximum wavelengths of the longest-wavelength absorption shifted from 398 nm to 486 nm. Likewise, the emission shifted to the region of orange emission. As in Figure S4, an isosbestic point was clearly observed at 434 nm, which was indicative of the formation of a 1:1 complex between **5c** and $B(C_6F_5)_3$. The emission at 488 nm gradually decreased (Figure S5), whereas the emission at 592 nm gradually increased (Figure S6).

Table 3. Addition of $B(C_6F_5)_3$ to the toluene solution of **5c**

| Thiazole | $\lambda_{abs}$ (nm)[a] | $\lambda_{ex}$ (nm) | $\lambda_{em}$ (nm)[a,b] | $\Phi_F$ | Stokes shift ($cm^{-1}$) [nm] | CIE[c] |
|---|---|---|---|---|---|---|
| 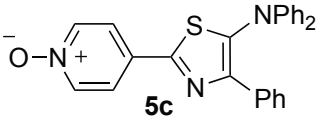 **5c** | 398 | 394 | 488 | 0.06 | 4634 [90] | (0.17, 0.31) |
| **5c**+$B(C_6F_5)_3$ (15 equiv) | 486 | 486 | 592 | 0.29 | 3684 [106] | (0.54, 0.45) |

[a] In toluene, [thiazole] = $1x10^{-5}$ M.
[b] Excited at $\lambda_{ex\ max}$. $\Phi_F$ corresponds to absolute fluorescence quantum yield.
[c] International Commission on Illumination (CIE) coordinates.

Finally, the photophysical properties of **5** in a solid state were elucidated (Table 4). The absorption and emission spectra of **5** in a solid state, except for **5d**, were observed in nearly the same regions as those in solution. The emission of **5d** was observed at 527 nm, which was blue-shifted compared to that in solution. More interestingly, grinding of **5d** shifted the emission to 599 nm, while other *N*-oxides **5a**–**5c** did not show a noticeable change. Increasing attention has been paid to mechanofluorochromism of low-molecular-weight organic molecules.[12] In particular, molecules that show drastic spectral shifts when subjected to grinding are desired. We examined the details of the mechanofluorochromism of **5d** by powder X-ray diffraction (XRD) (Figure 4). The diffraction pattern of XRD of unground solid **5d** showed many sharp and strong diffraction peaks, which reflect the crystalline nature of **5d**. In contrast, these peaks disappeared when **5d** was ground; instead, a broad peak was observed at around 20°. This suggests that **5d** underwent a phase transition from the crystalline state to the amorphous state by grinding. The change from yellow-green emission to orange emission was confirmed visually (Figure S7). The orange

emission of ground **5d** persisted at least overnight, whereas exposure of orange-colored sample to solvent vapors changed the color of the emission almost instantly. For example, when ground **5d** was exposed to acetone vapor, the color of the emission changed to yellow-green. The XRD pattern of the sample exposed to acetone vapor showed several sharp peaks (Figure 4, (c)), which indicates crystallization toward the original state. To further elucidate the solvent effects, ground **5d** was exposed to the vapors of a range of solvents such as cyclohexane, toluene, diethyl ether, THF, chloroform, dichloromethane, acetone, acetonitrile, and methanol (Table 5 and Figure S8). The absorption and emission spectra of the samples exposed to solvent vapors were nearly identical to those before grinding, except for methanol. A shift to a slightly longer wavelength was observed when samples were exposed to methanol vapor, with absorption at 472 nm and emission at 558 nm. This implies that a different crystalline state is formed only when the sample is exposed to methanol vapor. The XRD patterns of the samples exposed to a range of solvents also suggest this difference (Figure S9).

Table 4. Fluorescent spectra of *N*-oxides **5** in a solid state

| Thiazole | UV-vis[a] $\lambda_{abs}$ (nm) | $\lambda_{ex}$ (nm)[b] | $\lambda_{em}$ (nm)[b] | $\Phi_F$[b, c] | Stokes shift ($cm^{-1}$) [nm] |
|---|---|---|---|---|---|
| 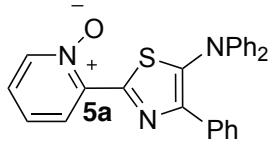 **5a** | 405 | 363 | 504 | 0.13 | 4850 [99] |
| 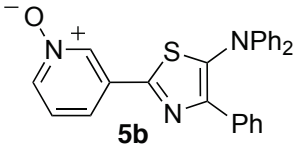 **5b** | 397 | 345 | 485 | 0.09 | 4570 [88] |
| 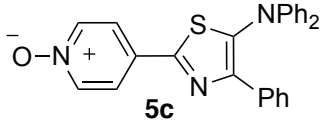 **5c** | 417 | 450 | 555 | 0.04 | 5963 [138] |
| 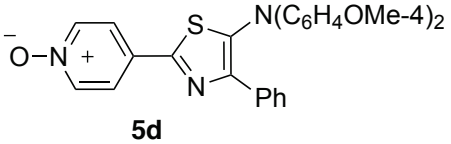 **5d** | 456<br>498[c] | 456<br>498[c] | 527<br>599[c] | 0.07<br>0.06[c] | 2955 [71]<br>3386 [101] |

[a] Measured on V-770.
[b] Measured on FP-8500.
[c] After grinding.

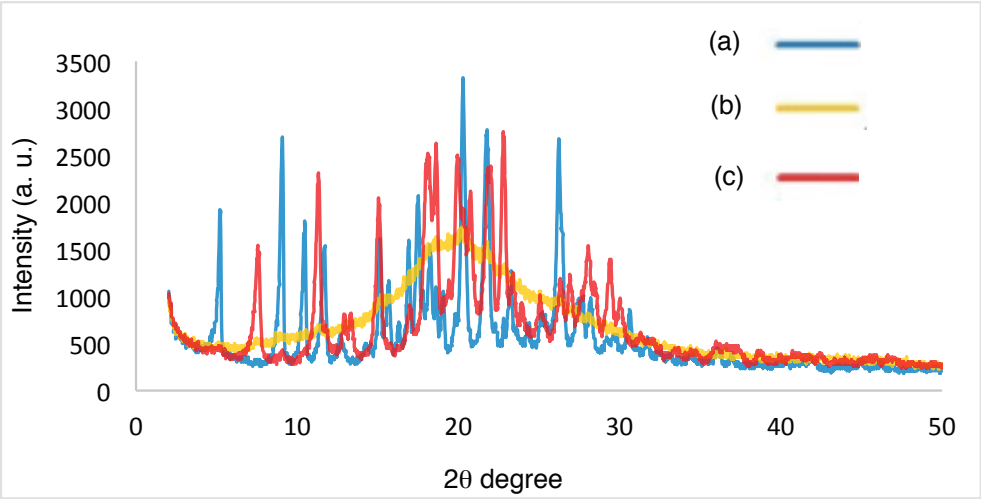


Figure 4. XRD patterns of **5d**: (a) before grinding, (b) after grinding, (c) after exposure to acetone

Table 5. UV-vis and fluorescence spectra of **5d** after exposure of the ground sample to a solvent

| solvent | $C_6H_{12}$ | toluene | $Et_2O$ | THF | $CHCl_3$ | $CH_2Cl_2$ | acetone | MeCN | MeOH | before grinding |
|---|---|---|---|---|---|---|---|---|---|---|
| $\lambda_{abs}$[a] (nm) | 457 | 457 | 457 | 457 | 472 | 457 | 457 | 457 | 472 | 456 |
| $\lambda_{em}$[b,c] (nm) | 547 | 544 | 543 | 548 | 548 | 548 | 548 | 547 | 558 | 527 |
| Stokes shifts | | | | | | | | | | |
| (nm) | 90 | 87 | 86 | 91 | 76 | 91 | 91 | 90 | 86 | 71 |
| ($cm^{-1}$) | 3600 | 3500 | 3466 | 3634 | 2938 | 3634 | 3634 | 3600 | 3265 | 2955 |

[a] Measured on V-770.
[b] Measured on FP-8500.
[c] Excited at $\lambda_{ex\ max}$.

## CONCLUSIONS

In summary, we have demonstrated the synthesis and properties of (5-amino-2-thiazolyl)pyridine *N*-oxides. The compounds were prepared in low to moderate yields by the oxidation of 2-pyridyl-5-aminothiazoles. The *N*-oxides showed absorption properties similar to those of the starting thiazoles, while the emission of the *N*-oxides was red-shifted by more than 24 nm. Among them, *N*-oxide **5d** showed emission in an orange region at 604 nm. More interestingly, *N*-oxide **5d** exhibited mechanofluorochromism. When **5d** was subjected to grinding, the emission shifted from 527 nm to 599 nm. XRD patterns indicated the formation of an amorphous state by the grinding. Further studies on thiazole-based fluorescent molecules are in progress.

## EXPERIMENTAL

**Supporting Information.** Experimental procedures, spectroscopic and analytical data for all new compounds including copies of NMR spectra.

## ACKNOWLEDGEMENTS

This work was supported by JSPS KAKENHI grants 18H04396 (Middle Molecular Strategy).

This paper is dedicated to Professor Kaoru Fuji on the occasion of his 80th birthday.

## REFERENCES AND NOTES

1. a) T. Murai, A. Yoshida, T. Mizutani, H. Kubuki, K. Yamaguchi, T. Maruyama, and F. Shibahara, *Chem. Lett.*, 2017, **46**, 1017; b) Y. Maekawa, K. Kuwabara, A. Sugiyama, K. Iwata, T. Maruyama, and T. Murai, *Chem. Lett.*, 2017, **46**, 1068; c) K. Kuwabara, Y. Maekawa, M. Minoura, and T. Murai, *Org. Lett.*, 2018, **20**, 1375 and references cited therein.
2. a) T. Murai, F. Hori, and T. Maruyama, *Org. Lett.*, 2011, **13**, 1718; b) K. Yamaguchi, T. Murai, S. Hasegawa, Y. Miwa, S. Kutsumizu, T. Maruyama, T. Sasamori, and N. Tokitoh, *J. Org. Chem.*, 2015, **80**, 10742; c) K. Yamaguchi, T. Murai, S. Kutsumizu, Y. Miwa, M. Ebihara, J.-D. Guo, and N. Tokitoh, *ChemistryOpen*, 2017, **6**, 282; d) T. Murai, K. Yamaguchi, T. Hayano, T. Maruyama, K. Kawai, and A. Yashita, *Organometallics*, 2017, **36**, 2552; e) T. Murai, H. Furukawa, and K. Yamaguchi, *Heterocycles*, 2018, **97**, 409; f) T. Murai, M. Yoshihara, K. Yamaguchi, and M. Minoura, *Asian J. Org. Chem.*, 2019, **8**, 1102.
3. K. Yamaguchi, T. Murai, J.-D. Guo, T. Sasamori, and N. Tokitoh, *ChemistryOpen*, 2016, **5**, 434.
4. K. Yamaguchi, T. Murai, Y. Tsuchiya, Y. Miwa, S. Kutsumizu, T. Sasamori, and N. Tokitoh, *RSC Adv.*, 2017, **7**, 18132.
5. As a rare example, 5-methoxythiazoles bearing pyridine *N*-oxide moieties at the 2-position are used for digital pH fluorescent sensing. Their emissions were observed from 385–450 nm. See: M.-H. Zheng, M.-M. Zhang, H.-H. Li, and J.-Y. Jin, *J. Fluoresc.*, 2012, **22**, 1421.
6. For recent reviews, see; a) S. Xue, X. Qiu, Q. Sun, and W. Yang, *J. Mater. Chem. C*, 2016, **4**, 1568; b) M. Krzeszewski, D. Gryko, and D. T. Gryko, *Acc. Chem. Rev.*, 2017, **56**, 2354; c) P.-Z. Chen, L.-Y. Niu, Y.-Z. Chen, and Q.-Z. Yang, *Coord. Chem. Rev.*, 2017, **350**, 196; d) C. Carayon and S. Fery-Forgues, *Photochem. Photobiol. Sci.*, 2017, **16**, 1020; e) Z. He, C. Ke, and B. Z. Tang, *ACS Omega*, 2018, **3**, 3267; f) J. Christoffers, *Eur. J. Org. Chem.*, 2018, 2366; g) S. Mukherjee and P. Thilagar, *Angew. Chem. Int. Ed.*, 2019, **58**, 7922.
7. T. Nishida, A. Fukazawa, E. Yamaguchi, H. Oshima, S. Yamaguchi, M. Kanai, and Y. Kuninobu,

*Chem. Asian J.*, 2014, **9**, 1026.

8. a) N. Mataga, Y. Kaifu, and M. Koizumi, *Bull. Chem. Soc. Jpn.*, 1956, **29**, 465; b) V. E. Z. Lippert, *Elektrochem.*, 1957, **61**, 962; c) N. Mataga and T. Kubota, *Molecular Interactions and Electronic Spectra*; Dekker: New York, 1970; d) E. L. Lippert, *Organic Molecular Photophysics*; Wiley: New York, 1975.
9. a) G. Haberhauer, R. Gleiter, and C. Burkhart, *Chem. Eur. J.*, 2016, **22**, 971; b) G. Haberhauer, *Chem. Eur. J.*, 2017, **23**, 9288.
10. For recent examples, see: a) F. Wang, C. A. DeRosa, M. L. Daly, D. Song, M. Sabat, and C. L. Fraser, *Mater. Chem. Front.*, 2017, **1**, 1866; b) T. N. Moshkina, E. V. Nosova, G. N. Lipunova, M. S. Valova, and V. N. Charushin, *Asian J. Org. Chem.*, 2018, **7**, 1080; c) F. Wang, D. Song, D. A. Dickie, and C. L. Fraser, *Chem. Asian J.*, 2019, **14**, 1849; d) A. Kundu, S. Karthikeyan, Y. Sagara, D. Moon, and S. P. Anthony, *ACS Omega*, 2019, **4**, 5147.
11. For recent examples, see: a) J. Tydlitat, S. Achelle, J. Rodríguez-Lopez, O Pytela,T. Mikysek, N. Cabon, F. R. Guen, D. Miklik, Z. Ruzickova, and F . Bures, *Dyes Pigm.*, 2017, **146**, 467; b) K. Imamura, Y.Ueno, S. Akimoto, K . Eda, Y. Du, C. Eerdun, M. Wang, K. Nishinaka, and A. Tsuda, *ChemPhotoChem*, 2017, **1**, 427.
12. For reviews, see: a) P.-Z. Chen, L.-Y. Niu, Y.-Z. Chen, and Q.-Z. Yang, *Coord. Chem. Rev.*, 2017, **350**, 196; b) C. Wang and Z. Li, *Mater. Chem. Front.*, 2017, **1**, 2714; c) W. Chen, Y. Pan, J. Chen, F. Ye, S. H. Liu, and J. Yin, *Chin. Chem. Lett.*, 2018, **29**, 1429; d) X. Huang, L. Qian, Y. Zhou, M. Liu, Y. Cheng, and H. Wu, *J. Mater. Chem. C*, 2018, **6**, 5075; e) P. Data and Y. Takeda, *Chem. Asian J.*, 2019, **14**, 1613.